

This article was downloaded by:

On: 25 January 2011

Access details: *Access Details: Free Access*

Publisher *Taylor & Francis*

Informa Ltd Registered in England and Wales Registered Number: 1072954 Registered office: Mortimer House, 37-41 Mortimer Street, London W1T 3JH, UK



Liquid Crystals

Publication details, including instructions for authors and subscription information:

<http://www.informaworld.com/smpp/title~content=t713926090>

Synthesis and mesomorphic properties of some new chiral thiobenzoates containing three rings

M. D. Ossowska-Chruściel^a

^a Institute of Chemistry, University of Podlasie, 08-110 Siedlce, Poland

To cite this Article Ossowska-Chruściel, M. D.(2007) 'Synthesis and mesomorphic properties of some new chiral thiobenzoates containing three rings', *Liquid Crystals*, 34: 2, 195 – 211

To link to this Article: DOI: 10.1080/02678290601116217

URL: <http://dx.doi.org/10.1080/02678290601116217>

PLEASE SCROLL DOWN FOR ARTICLE

Full terms and conditions of use: <http://www.informaworld.com/terms-and-conditions-of-access.pdf>

This article may be used for research, teaching and private study purposes. Any substantial or systematic reproduction, re-distribution, re-selling, loan or sub-licensing, systematic supply or distribution in any form to anyone is expressly forbidden.

The publisher does not give any warranty express or implied or make any representation that the contents will be complete or accurate or up to date. The accuracy of any instructions, formulae and drug doses should be independently verified with primary sources. The publisher shall not be liable for any loss, actions, claims, proceedings, demand or costs or damages whatsoever or howsoever caused arising directly or indirectly in connection with or arising out of the use of this material.

Synthesis and mesomorphic properties of some new chiral thiobenzoates containing three rings

M. D. OSSOWSKA-CHRUŚCIEL

Institute of Chemistry, University of Podlasie, 3-go Maja 54, 08-110 Siedlce, Poland; e-mail: dch@ap.siedlce.pl

(Received 1 March 2006; in final form 28 August 2006; accepted 18 September 2006)

Six new compounds with chiral terminal chains and three rings bridged via the –COS– and –COO– groups have been synthesized. Three of them belong to series **A** and have two benzene rings and one bicyclo[2,2,2]octane, while the remaining three come from series **B**, where all three are benzene rings. Series **A** compounds share a characteristic feature of two smectic phases: SmA* and SmB*, whereas mesogens from the **B** series exhibit only the one SmA* phase.

1. Introduction

In a conventional molecule of a thermotropic liquid crystal, replacement of one phenyl ring by the bicyclo[2,2,2]octane group almost always extends the temperature range of the mesophase. In some cases it induces a new phase similar to the one presented in this work. Gray and Kelly [1, 2] and Carr and Gray [3, 4] reported different types of mesogens with bicyclo[2,2,2]octane and cyanophenyl groups. These homologues have higher clearing temperatures than their benzene analogues. Similar results were presented for derivatives of compounds with bicyclo[2,2,2]octane with a cyano terminal group [5]. The change of polymorphism in bi-, tri- and tetra-substituted liquid crystals with an ethyl central group has been shown previously [6, 7]. The increase in mesophase temperature range was also observed in these cases. Melting temperature was found to decrease by as much as 86°C, with only a slight lowering of clearing temperature (by 5°C) [8]. The introduction of thioester into an ester group leads to an increase in both melting and clearing temperatures.

Achiral liquid crystal compounds with a bicyclo[2,2,2]octane ring and the central bridge have also been previously described [1–8]. Mesogens with the bicyclo[2,2,2]octane ring, as components of mixtures, cause a decrease in viscosity and lead to the creation of new phases [5, 7]. In the search for new liquid crystalline materials useful as components of mixtures, new three-ring chiral mesogens from the **A** and **B** series have been synthesized. The chemical structures of chiral mesogens from these series are presented in figure 1.

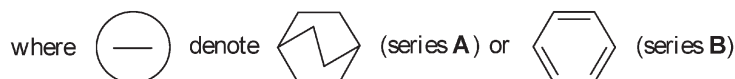
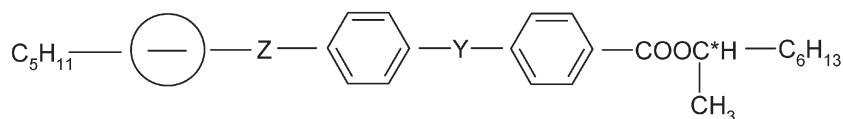
Each of these six compounds has a chiral terminal chain but none of their smectic phases shows any electro-optical switching, even at high voltages. Both

the thioester link and its position in the molecule have an important influence on the mesomorphic properties of liquid crystals; the presence of the bicyclo[2,2,2]octane ring also influences the phase transitions. The compounds from series **A** with the –COO– central groups have an enantiotropic SmA* and monotropic SmB* phases, while mesogens with the –COS– central group have enantiotropic SmA* and SmB* phases. A characteristic feature of the series **B** compounds is the occurrence of only one enantiotropic SmA* phase. As will be shown later, this difference in the location of the –COS– and –COO– central groups induces significant changes in the phase behaviour.

2. Characterization

The structures of the final products and of the intermediates were confirmed by IR and ¹H NMR spectroscopy and by elemental analysis (EA). The ¹H NMR spectra were obtained on a Varian Unity Plus spectrometer operating at 200 MHz or 500 MHz (CDCl₃, TMS as internal standard). IR spectra were recorded on a FTIR Nicolet Magna 760 spectrometer. The chemical purity was checked by thin layer chromatography and further confirmed by elemental analysis using a Perkin-Elmer 2400 spectrometer. The optical purity of compounds was determined by chiral HPLC.

Transition temperatures were determined by means of a polarizing microscope with Linkam programmable heating stage THMSE 600. Heating and cooling rates were ± 2 K min⁻¹. DSC measurements were performed using a DSC 822^c Mettler Toledo Star System differential scanning calorimeter. The transition temperatures were also examined by polarized optical



and Z and Y are respectively:

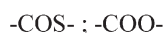
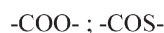
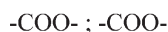


Figure 1. The chemical structures of chiral mesogens from the **A** and **B** series.

microscopy (POM) and transmitted light intensity (TLI) methods. X-ray measurements were performed on a Philips X'Pert diffractometer as well as a Guinier symmetrical focusing transmission photographic camera. The ordinary and extraordinary refractive indices (n_o and n_e) of all compounds from the **A** and **B** series were measured with the Atago-2T refractometer at sodium wavelength ($\lambda_{Na} = 5893 \text{ \AA}$).

3. Synthesis

In the chemical structures of chiral mesogens from the **A** and **B** series there are certain regular molecular fragments, namely: 4-pentylbicyclo[2,2,2]octyl (series **A**, **6**, **8** and **10**) and 4-pentylphenyl (series **B**, **7**, **9** and **11**), and a chiral chain (**A** and **B** series). Compounds from the **A** and **B** series were prepared according to the procedures presented in detail in Figure 2.

Synthesis of the triesters **6–11** began with the preparation of the hydroxy-diester intermediates **3** and **4** and mercapto-diester **5**. (*S*)-(+)-1-methylheptyl 4-(4-hydroxybenzoyloxy)benzoate **3** was obtained according to the general methods shown in figure 3. The (*S*)-(+)-2-octanol was purchased from Fluka Co. Chem., chira select >99.5%. The intermediates 1-methylheptyl 4-hydroxybenzoate **17** and **3** were also obtained with chira select 99.5% (HPLC) (m.p. 45.5°C). The hydroxy-diester **3** was obtained by esterification of compound **17** with compound **14**, and the product **18** was deprotected by hydrogenolysis to the hydroxy-diester **3**.

Hydroxy-diester **4** was prepared by the procedure presented in figure 4, through a modification of the method already described for other systems [9–12].

4-Mercaptobenzoic acid **19** was a starting substance. Under slow oxidation it was transformed into dithiodibenzoic acid **20**. The acid chloride **21** was obtained by the usual method. Compound **21** was isolated from the reaction mixture by extraction with hot hexane and was purified by double recrystallization from hexane. The diester dithiodibenzoic acid **22** was prepared by esterification of **21** with (*S*)-(+)-2-octanol in the presence of toluene and pyridine; it was purified by flash chromatography. The dithiol group was then reduced with sodium borohydride in absolute ethanol under nitrogen, and the resulting (*S*)-(+)-1-methylheptyl 4-mercaptobenzoate **23** was purified by flash chromatography under argon. The final product was obtained as a bright oil, purity 99.3% (HPLC). Compound **24** was prepared by reaction of **23** with 4-methoxycarbonyloxybenzoyl chloride in toluene and pyridine (1.05 mol/1.0 mol chloride) at 35–40°C, for 4 h. The thioester **24** was isolated and purified. Deprotection of the hydroxy group of **24** was performed by modified literature methods [3], to give compound **4**. Best results were obtained when the reaction was performed at 10°C, for 1.5 h and using an excess of NH_3aq 2.5 m/m.

The preparation of (*S*)-(+)-1-methylheptyl 4-(4-mercaptobenzoyloxy) benzoate **5** was carried out as shown in figure 5. Esterification of dithiodibenzoyl chloride **21** with the 1-methylheptyl 4-hydroxybenzoate **17** gave the desired disulphide **25**. Compound **5** was obtained by the reduction of **25** with sodium borohydride in isopropyl alcohol, with purification by column chromatography under dry argon. The final products **6–11** were prepared in the same way (figure 2) with satisfactory yields (68–75%).

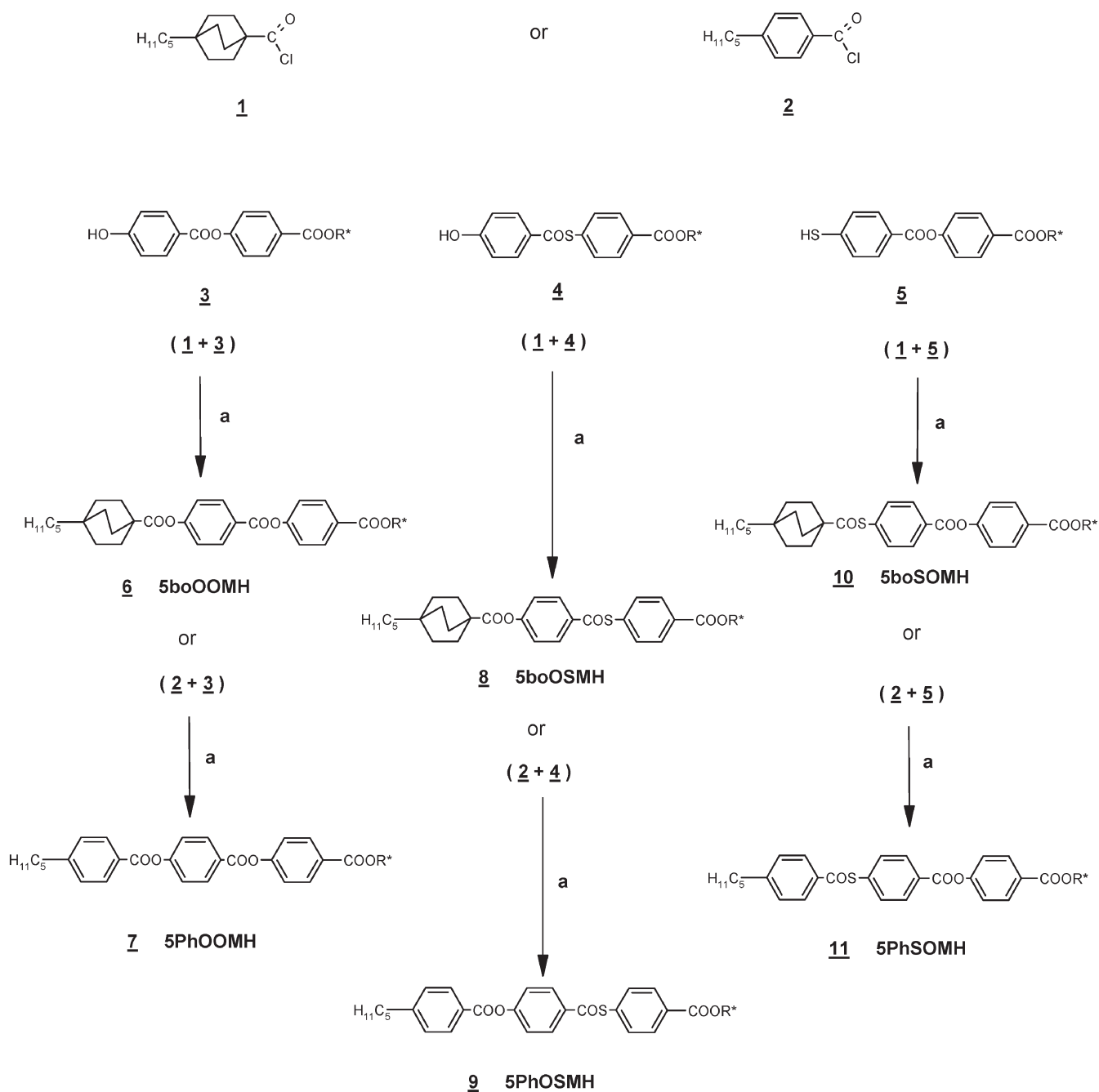


Figure 2. Synthesis route for compounds **6–11** (**6**, **8**, **10** series **A**, and **7**, **9**, **11** series **B**). R^* : (*S*)-(+)-1-methylheptyl group; a: pyridine, toluene.

All compounds, intermediate and final, were purified by column chromatography and crystallization until their melting point was constant.

4. Results and discussion

Differential scanning calorimetry (DSC), X-ray diffraction (XRD), FTIR spectroscopy, polarizing optical

microscopy (POM), transmitted light intensity (TLI) and measurements of specific conductivity (SC) and the ordinary and extraordinary refractive indices (RI) were used to study the thermal behaviour of all the liquid crystals from the **A** and **B** series. The phase behaviour was examined during heating and cooling at 2 K min^{-1} . Transition temperatures and associated enthalpy and entropy changes for compounds **6–11** obtained during

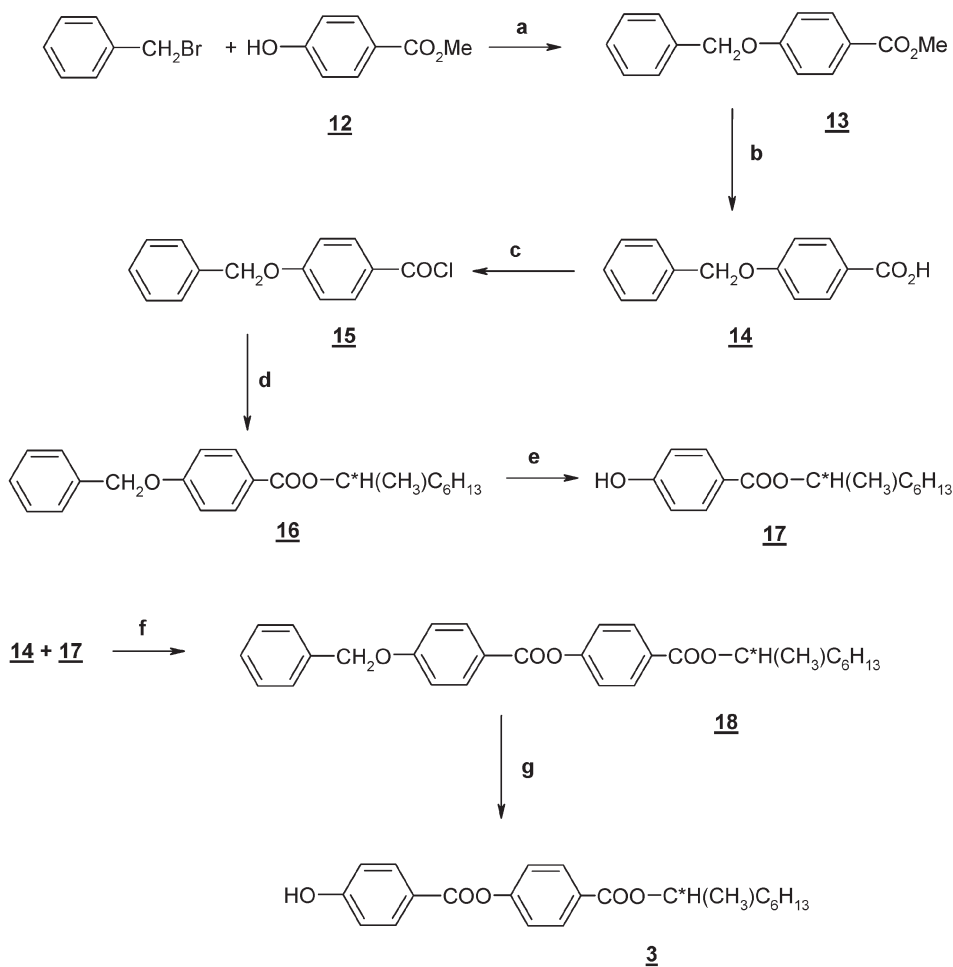


Figure 3. Synthesis route for compound **3**. a: NaOH, DMF/C₆H₆; b: NaOH(aq)/C₂H₅OH, HCl(aq); c: SOCl₂, toluene; d: (S)-(+)-HO-C*H(CH₃)C₆H₁₃, toluene, pyridine; e: H₂, 10% Pd-C, THF, 25–30°C; f: DCC, DMAP, CH₂Cl₂; g: H₂, 10% Pd-C, THF, 25–35°C.

heating are presented in table 1. Our studies showed that the mesophases of compounds from the **A** and **B** series showed no electro-optical switching, even at high voltages. From XRD and miscibility data, these compounds adopted only two phases: SmA* and SmB*, respectively.

Temperature ranges of the above-mentioned SmA* and SmB* phases are presented in figure 6. We see that: $\Delta T_{\text{SmA}} = T_{\text{Cr-SmA}} - T_{\text{SmA-I}}$ for **7**, **9**, **11** and **6**; $\Delta T_{\text{SmA+SmB}} = T_{\text{Cr-SmB}} - T_{\text{SmA-I}}$ for **8** and **10** possess different ranges of the SmA* and SmB* phases. The –COS– and –COO– positions between the rings influence the phase behaviour. When the –COS– group appears directly at the phenyl ring, the range of the SmA phase is greater than when it is located at the chiral branched group for the ternary phenyl system ($\Delta T_{\text{SmA}} = 19.0, 43.8$ and 63.8°C for **7**, **9** and **11**, respectively). The substitution of one bicyclo[2,2,2]octane ring for one of the three phenyl rings, as well as the introduction

of –COS– between rings, considerably extends the mesophase range ($\Delta T_{\text{SmA+SmB}} = 85.8$ and 88.8°C for **10** and **8**, compounds from the **A** series, figure 6 and table 1). During cooling, the SmB* phase in the 5boSOMH compound shows extensive supercooling and forms a glassy SmB state. No such behaviour is observed in 5boOSMH; it is probably caused by structural differences between these two compounds.

Interlayer distances were determined from X-ray measurements for all the studied liquid crystals. Sample results are given in figures 7 and 8 for temperature dependence of the layer spacing d for 5boSOMH (**10**) and 5boOSMH (**8**), respectively. The change of layer spacing d correlates with the temperature and enthalpy changes of the phase transition points SmB*–SmA*. As can be seen from figures 7 and 8, the interlayer distances for the SmB* and SmA* phases of **10** and **8** depend on the position of –COS– and –COO– in the molecules. In **10**, interlayer spacing d changes

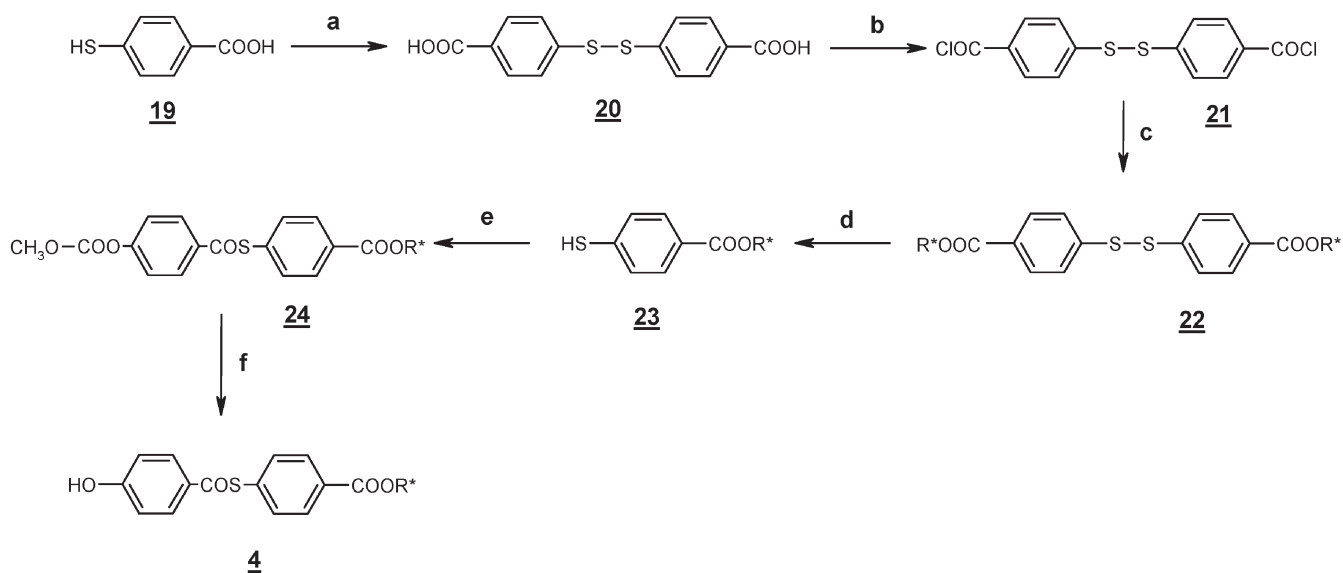


Figure 4. Synthesis route for compound **4**. R^* : (S)-(+)-1-methylheptyl group; a: NaOH (aq), I_2 , HCl; b: $SOCl_2$; c: (S)-(+)-2-octanol, toluene, pyridine; d: $NaBH_4$, ethanol; e: 4-methoxycarbonylbzoyl chloride, pyridine, CH_2Cl_2 ; f: NH_3 28%, isopropanol.

abruptly at the SmB^* - SmA^* phase transition (from 34.00 Å in SmB^* to *c.* 33.25 Å in SmA^*). In addition, d remains almost constant in the SmB phase until the T_{B-A} temperature is reached and then decreases slowly in the SmA^* phase.

In compound **8**, the SmB interlayer distance decreases slightly from 34.28 to 33.60 Å around the T_{B-A} temperature. In this case the $-COS-$ group is connected to the benzene ring in the vicinity of the chiral branched chain (S)-1-methylheptyloxy. The layer spacing d of the SmA^* phase is almost constant for 5boOSMH, in contrast to the behaviour of in 5boSOMH. The nature

of the changes in the layer spacing in the SmA^* phase of 5boSOMH and in the SmB^* of 5boOSMH indicates the existence of pretransition effects in these SmA^* and SmB^* phases. The only difference in chemical structure between **10** and **8** is the position of the $-COS-$ group. Hence this is the factor that influences the smectic layer thickness and the way it changes in the studied SmA^* and SmB^* phases. The values of the smectic layer spacing d measured in figure 9. The largest is in the SmA^* phase of the chiral thiobenzoate liquid crystal with three benzene rings, 5PhSOMH **11**, as compared with the

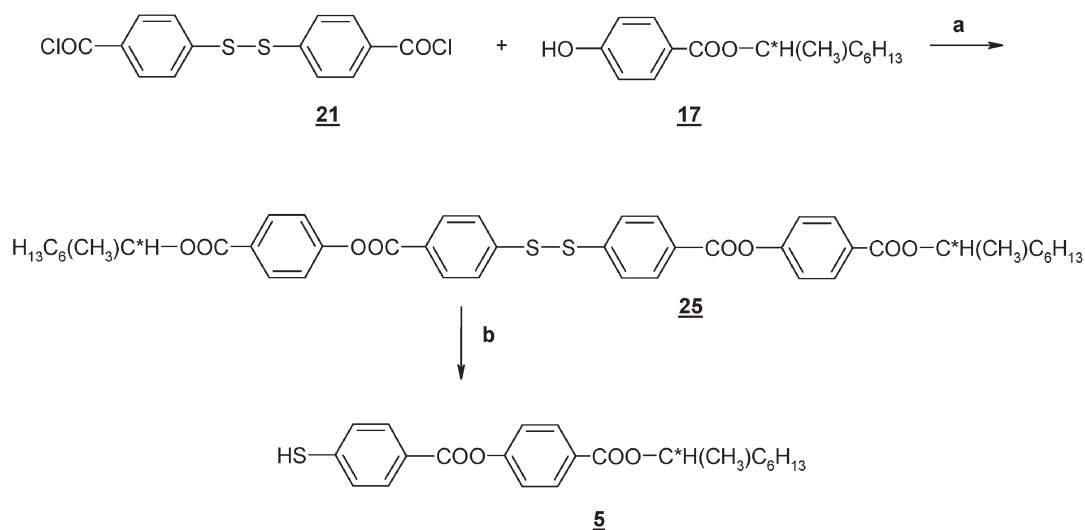


Figure 5. Synthesis of intermediate compound **5**. a: toluene, pyridine; b: $NaBH_4$, ethanol, N_2 .

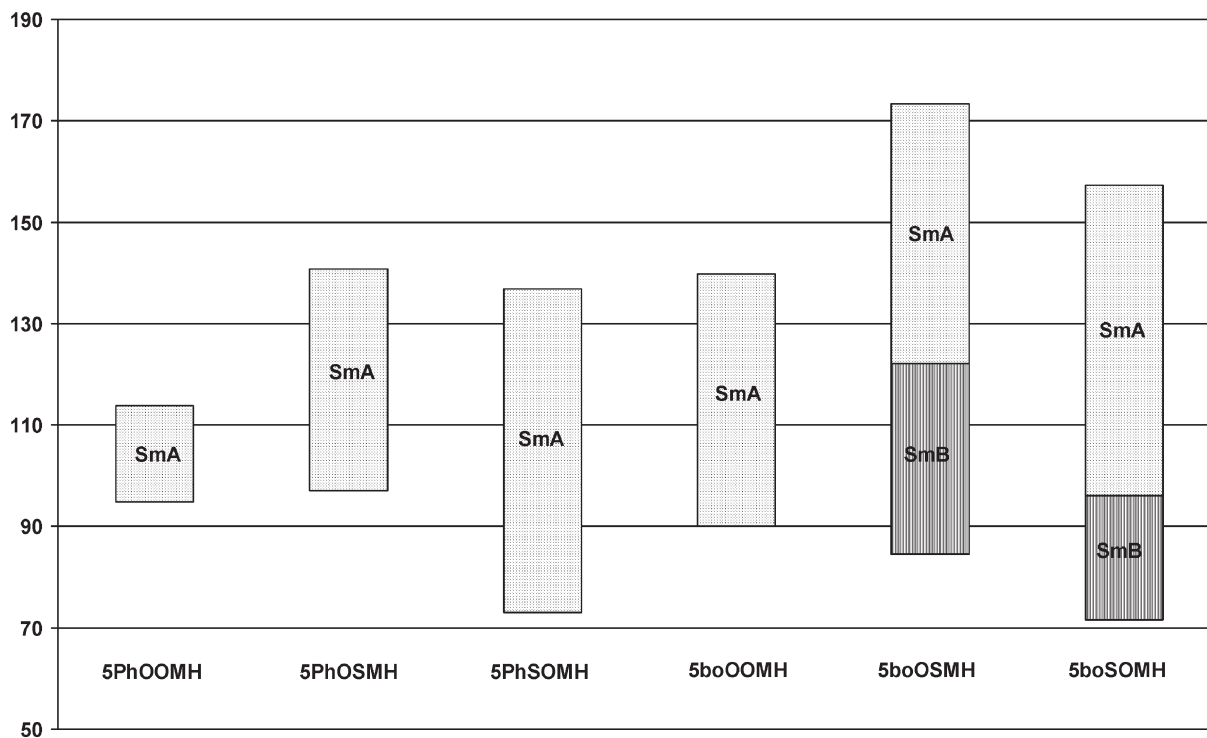
Table 1. Thermodynamic parameters characterizing phase transitions of compounds of the **A** and **B** series.

Compound	Parameters	Cr–SmB	Cr–SmA	SmB–SmA	SmA–I	ΔT
5boOOMH (6)	ΔH (kcal mol ⁻¹)	—	8.4	—	1.1	49.8
	T_p (°C)	—	90.0	—	139.8	
	ΔS (cal mol ⁻¹ K ⁻¹)	—	23.0	—	2.5	
5boOSMH (8)	ΔH (kcal mol ⁻¹)	6.1	—	0.5	1.1	88.8
	T_p (°C)	84.6	—	122.1	173.4	
	ΔS (cal mol ⁻¹ K ⁻¹)	17.0	—	1.2	2.5	
5boSOMH (10)	ΔH (kcal mol ⁻¹)	5.5	—	0.4	1.0	85.8
	T_p (°C)	71.5	—	96.0	157.3	
	ΔS (cal mol ⁻¹ K ⁻¹)	16.0	—	1.0	2.3	
5PhOOMH (7)	ΔH (kcal mol ⁻¹)	—	7.1	—	1.2	19.0
	T_p (°C)	—	94.8	—	113.8	
	ΔS (cal mol ⁻¹ K ⁻¹)	—	19.2	—	3.1	
5PhOSMH (9)	ΔH (kcal mol ⁻¹)	—	8.4	—	1.3	43.8
	T_p (°C)	—	97.0	—	140.8	
	ΔS (cal mol ⁻¹ K ⁻¹)	—	22.7	—	3.2	
5PhSOMH (11)	ΔH (kcal mol ⁻¹)	—	6.8	—	1.3	63.8
	T_p (°C)	—	73.0	—	136.8	
	ΔS (cal mol ⁻¹ K ⁻¹)	—	19.7	—	3.1	

values found for SmA* and SmB* of chiral three-rings thiobenzoates with a bicyclo[2,2,2]octane ring (5boOSMH **8** and 5boSOMH **10**).

For compounds where the –COS– group is close to the terminal chiral branched group (**9** and **8**), the layer spacings d of the SmA* and SmB* are larger than for **10**, where it neighbours the bicyclooctane ring (figure 9). In

the compound with two –COO– bridges, **6**, the SmA* layer spacing is the smallest. The determined differences between average interlayer distances (Δd_{avg}) of SmB* ($d_{\text{avg}}\text{SmB}^*$) and SmA ($d_{\text{avg}}\text{SmA}^*$) phases are the following: $\Delta d_{\text{avg}} = d_{\text{avg}}(\text{SmB}^*) - d_{\text{avg}}(\text{SmA}^*) = 0.66 \text{ \AA}$ for 5boOSMH **8**, and 0.71 \AA for 5boSOMH **10**. This leads us to the conclusion that this small change (on average c

Figure 6. Phase diagram for compounds of the **A** and **B** series.

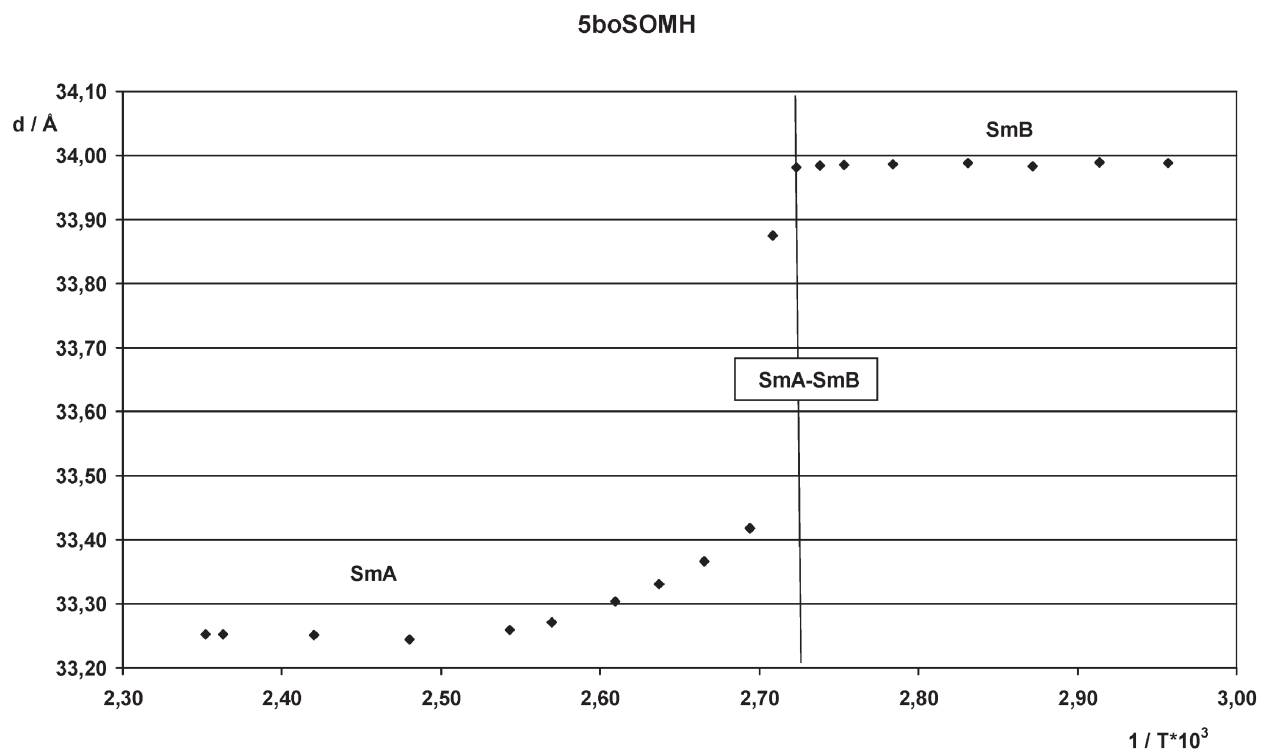


Figure 7. Temperature dependence of layer spacing d for 5boSOMH (10) obtained during cooling.

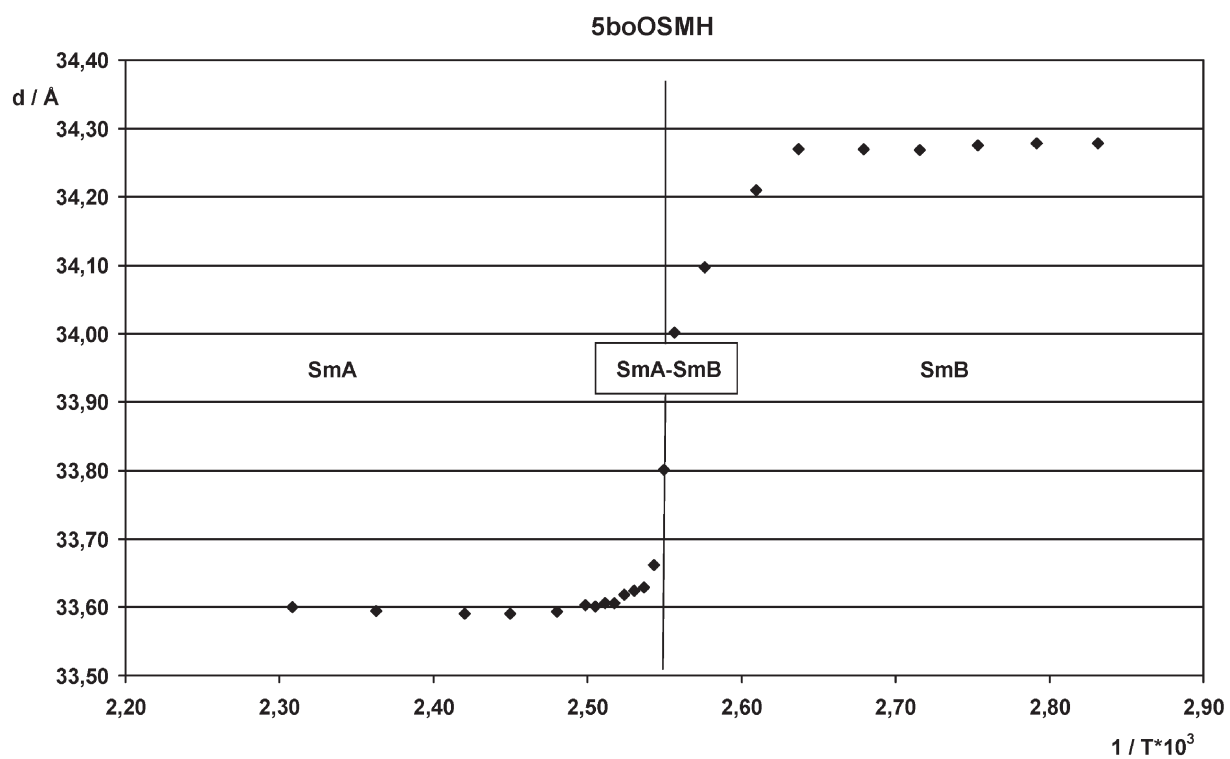


Figure 8. Temperature dependence of layer spacing d for 5boOSMH (8) obtained during cooling.

5PhSOMH, 5PhOSMH, 5PhOOMH, 5boOSMH, 5boSOMH and 5boOOMH

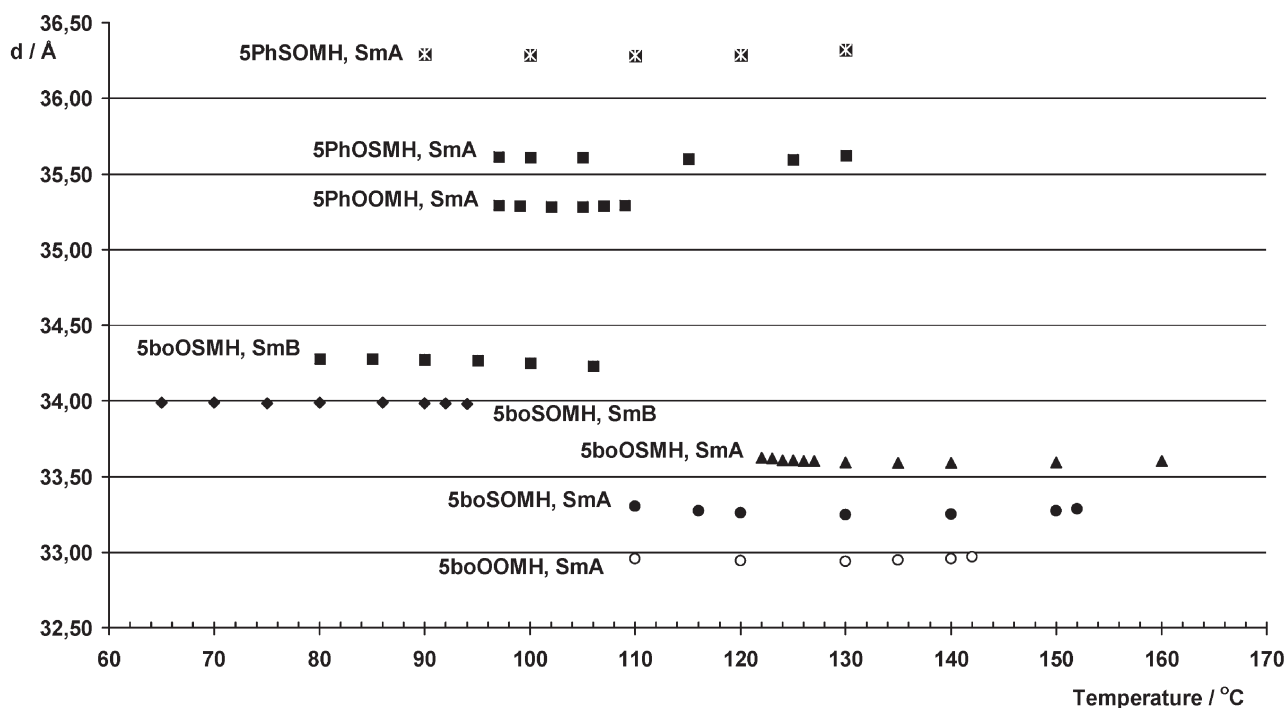


Figure 9. A comparison of the layer spacing d between the SmA* and SmB* phases.

2% for **8** and **10**) in the phase transition between two orthogonal phases, indicates a 'loose' structure inside a layer of the SmB* phase.

We have recently reported the crystal structure of a thioester from the homologous series of 4-*n*-pentylphenyl 4-*n*-alkoxythiobenzoates (*n*OS5) [14–16]. It is worth noting, that an all-*trans* conformation for alkyl and alkoxy chain is characteristic for the molecules of the *n*OS5 series. Theoretical calculations for the investigated molecule were carried out by the semiempirical MNDO3 method; the results are shown in figure 10, as an example for molecules of **8** (with bicyclo[2,2,2]octane ring) and **9** (with three phenyl rings). The net charge of the 5boOSMH and 5PhOSMH molecules shows two dipole groups, $-\text{COO}^-$ and $-\text{COS}^-$ in the central part, and one, $-\text{COOC}^*\text{H}(\text{CH}_3)\text{C}_6\text{H}_{13}$, in the terminal chain. The largest negative charges appear at oxygen atoms O1, O2, O3, O4 and O5 whereas the sulphur atom S1 has a slight positive charge. The angle between the terminal chiral group and the nearest phenyl plane is at *c.* 90° in both compounds.

It follows from crystallographic investigations of other liquid crystals that the chiral branched terminal chain (S)-1-methylheptyloxy and the nearest phenyl plane are tilted with respect to each other by *c.* 90° [17, 18]. This is also the case for molecular structures of the

other molecules studied. Table 2 presents a comparison of selected bond lengths and angles of 5boOSMH and 5PhOSMH in the central part of the molecules (thioester group with two adjacent benzene rings) and 4OS5 [16], 5OS5 [14] and 6OS5 [15], obtained from crystal structure analysis. It can be seen that the bond lengths and angles are comparable. This would justify the assumption that the calculated distances, and the molecular lengths in particular, should be close to the crystallographic values.

Interlayer distances d derived from X-ray measurements are given in table 3. In the SmA* phase of **6**, **8** and **10** (molecules with a bicyclooctane ring), d is comparable to the actual molecular lengths l calculated in their fully extended conformations, including the covalent radii of the H atoms, approximately 1.07 ($d/l=1.07$). For molecules of **7**, **9** and **11** (three benzene rings), $d/l=1.15$ and is greater than for **6**, **8** and **10**. This indicates the presence of a smectic structure of the SmA_{1e} subtype. Such SmA* phases are called enhanced monolayer SmA₁ phases [19]. Therefore compounds **6–11** will find better conditions for dimerization in the SmA_{1e} phase than in SmA₁. It may be expected that in **6–11** this occurs, as shown in figure 10.

TLI and POM measurements were carried out at a rate of $\pm 2 \text{ K min}^{-1}$ for all the compounds. As an

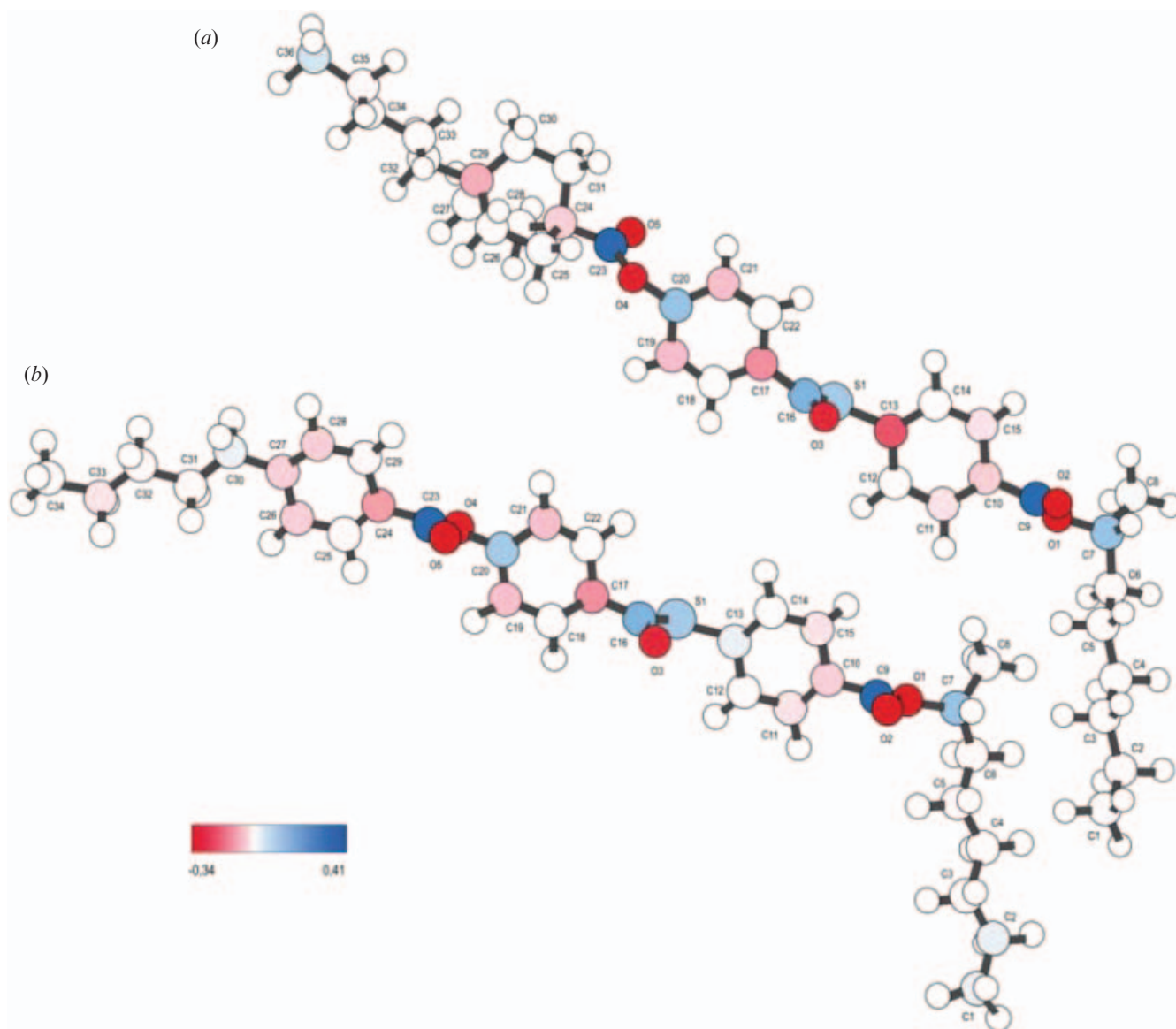


Figure 10. Molecular models of 5boOSMH and 5PhOSMH.

example, below are presented all the phase transitions observed by TLI and POM for 5boOSMH in two types of measurement cells: (1) microslide without alignment layers, glued with cover glass with constant thickness $c. 10 \mu\text{m}$ (classical cell) and (2) $5 \mu\text{m}$ thick measuring cell, coated with aligning polyamide layer, HG, produced by Linkam. The value of our home made TLI set-up for the studies of phase polymorphism has been discussed elsewhere [20]. The TLI curves obtained for 5boOSMH during heating and cooling are shown in figure 11 (Linkam cell). Clear differences are visible upon the transitions from isotropic to SmA*, from SmA* to SmB* and from SmB* to crystal. The Cr–SmB*, SmB*–SmA* and SmA*–I transition temperatures are

consistent with results obtained by other methods (DSC and POM). Note that figure 11 shows the same solid phase during heating and cooling as well as the supercooling effect of the SmB* phase. The TLI curves obtained for cell type (2) show that the phase transitions are less clearly visible than in cell type (1). In the two cells the phase transitions temperatures were almost identical.

Figure 12 presents distinctly different textures of the three phases (SmA*, SmB* and Cr), obtained for the two types of measurement cell, as observed by POM during cooling. Analysis of the texture simplifies the identification and assignment of each of these phases to changes observed in TLI. Figures 12 (a–e) classical and

Table 2. A comparison bond lengths (Å) and angles (°) of 5boOSMH and 5PhOSMH (calculated) and 4OS5 [16], 5OS5 [14] and 6OS5 [15] (crystal structure).

	5boOSMH	5PhOSMH	4OS5	5OS5	6OS5
<i>Bond length</i>					
C(16)–S(1)	1.781	1.781	1.768	1.785	1.746
S(1)–C(13)	1.762	1.763	1.769	1.772	1.785
O(3)–C(16)	1.228	1.227	1.198	1.211	1.215
C(16)–C(17)	1.506	1.505	1.476	1.481	1.470
<i>Angles</i>					
C(16)–S(1)–C(13)	109.3	108.9	103.0	102.4	102.6
S(1)–C(16)–O(3)	122.2	122.1	121.7	121.5	121.5
O(3)–C(16)–C(17)	122.2	122.2	124.5	124.2	123.8
S(1)–C(16)–C(17)	115.5	115.7	114.8	114.3	114.7
C(16)–C(17)–C(22)	119.9	120.1	120.0	122.2	122.9
C(16)–C(17)–C(18)	120.9	120.7	123.2	118.6	118.7
C(22)–C(17)–C(18)	119.0	119.0	118.3	119.2	118.4
S(1)–C(13)–C(12)	121.7	120.9	121.5	121.2	121.2
S(1)–C(13)–C(14)	119.3	120.0	119.8	118.6	122.2

(a' - e') HG Linkam, demonstrate: (a) SmA*, fan-shaped texture with focal-conics at 161.5°C; (a') SmA*, ordered fan-shaped texture at 161.5°C; (b) phase transition SmA*–SmB* with decreasing temperature at 121.7°C; (b') beginning of phase transition SmA*–SmB* at 121.7°C; (c) SmB*, from fan-shaped texture with diminished number of discontinuities at 118.7°C; (c') SmB*, obtained from SmA* at 118.7°C; (d) beginning of phase transition SmB*–Cr at 39.6°C; (d') phase transition SmB*–Cr at 39.6°C; (e) solid state, paramorphosis from SmB* with spherulitic regions at 27.0°C; (e') solid state, paramorphic texture obtained by cooling SmB* at 27.0°C.

The use of two types of cell confirms that whether the cell surface is aligned or unaligned does indeed influence the textures obtained. Thus TLI and POM once again proved useful as research methods in the study of polymorphism, and provided complementary information to DSC.

Temperature variations of optical birefringence (Δn) of 5PhOSMH **9** from series **B** and of two compounds from series **A** are shown in figures 13–15. The value of Δn decreases quite quickly with temperature from 0.174

to 0.162 in the vicinity of the SmA*–I phase transition for **9** (figure 13). Much the same changes of optical birefringence were observed for other chiral thiobenzoates **7** and **11** containing three benzene rings. As is evident from figures 14 and 15, the optical birefringence Δn of compounds with bicyclooctane rings, 5boOSMH **8**, and 5boSOMH **10**, is much smaller than that of **9** (in **8** $\Delta n=0.135$ and in **9** $\Delta n=0.174$ – 0.162). For 5boOSMH, Δn is constant in SmA* ($\Delta n=0.135$) and changes abruptly at the SmA*–SmB* transition; it then increases linearly very slowly in the SmB* phase (figure 14). For 5boSOMH, Δn distinctly increases in SmA* and is almost linear in the SmB* phase. A small pretransitional effect in the optical birefringence of 5boSOMH is also observed in the change of the layer spacing d (figure 7).

The similar behaviour of specific conductivity σ vs. reciprocal temperature for 5boSOMH and 5boOSMH is shown in figure 16. The only distinct changes to be seen are those corresponding to the SmA*–SmB* phase transition in 5boOSMH. The specific conductivity between the SmA* and SmB* phases cannot be clearly separated from that of the SmA* and SmB* phases for 5boSOMH. In general, specific conductivity within the SmA* phase decreases very slowly, and is almost constant in the SmB* phase.

Table 3. Interlayer distance d in the SmA* phase and calculated molecular length l as a function of the molecular structure.

Compound	$d/\text{Å}$	$l/\text{Å}$	d/l
5boOOMH (6)	32.97	31.02	1.06
5boOSMH (8)	33.60	31.33	1.07
5boSOMH (10)	33.27	31.21	1.07
5PhOOMH (7)	35.29	30.69	1.15
5PhOSMH (9)	35.61	30.90	1.15
5PhSOMH (11)	36.29	31.28	1.16

5. Preparation of materials

5.1. (S)-(+)-1-Methylheptyl 4-benzyloxybenzoate, **16**

(S)-(+)-2-Octanol (0.01 mol) was added dropwise at room temperature to a solution of 4-benzyloxybenzoyl chloride **15** (0.01 mol) and pyridine (0.02 mol) in dry toluene (50 ml), with vigorous stirring. The reaction mixture was then stirred at 35–40°C for 15 h and the

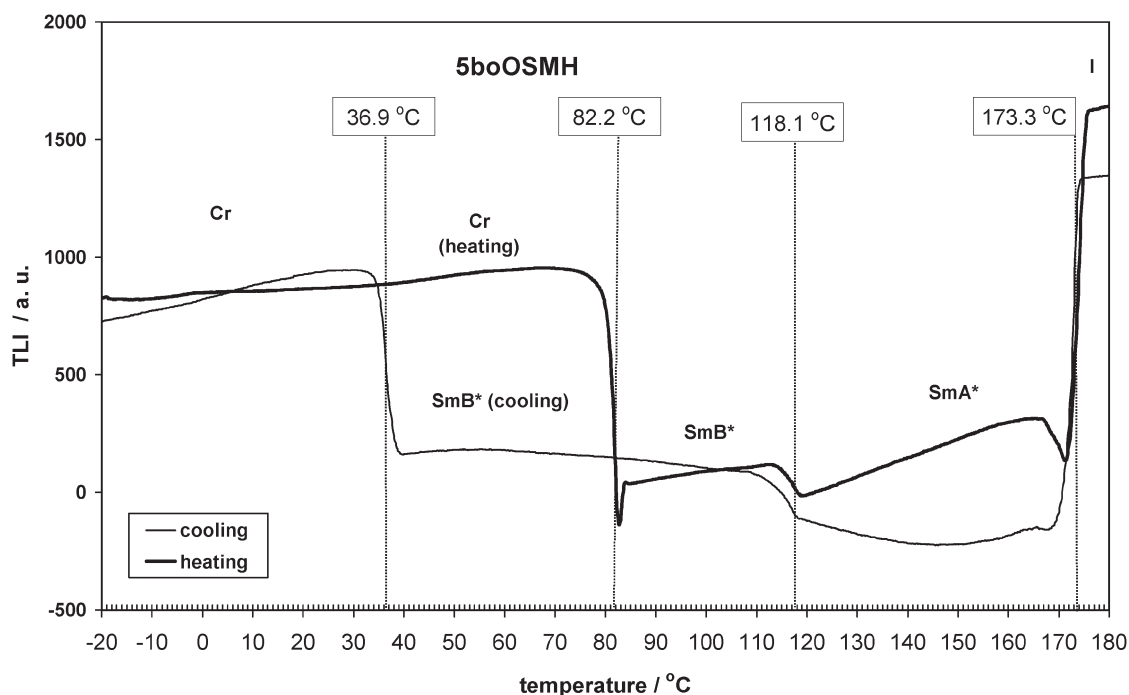


Figure 11. TLI curve for 5boOSMH for heating (thick line) and cooling (thin line).

progress of the reaction was monitored by TLC. The reaction mixture was neutralized with cold 5% aqueous HCl. The organic phase was separated, washed with water, aq. Na₂CO₃, again water, then dried over anhydrous MgSO₄. The solvent was removed and the crude material purified by flash chromatography using 60–100% CH₂Cl₂ in hexane. At room temperature the product was a pale yellow oil, yield 86.8%, m.p. 24°C. ¹H NMR (500 MHz, CDCl₃): δ(ppm) 0.95–0.86(m,6H,2-CH₃); 1.38–1.31(m,16H,-CH₂-); 1.60–1.65(m,3H,-C*-CH₃); 3.90(s,2H,-CH₂-O-); 4.52(s,1H,-C*-H); 7.15–7.27(m,5H,-ArH); 7.65–8.06(2d, 4H,-ArH). MS: *m/z* 340 λ₁ (M⁺); 211 λ₂; 120 λ₃; 91 λ₄; 65 λ₅. IR (KBr) (cm⁻¹): 3081; 3039; 2950; 2941; 1725; 1706; 1600; 1560; 1490; 1400.

5.2. (S)-(+)-1-Methylheptyl 4-hydroxybenzoate, 17

A solution of the benzyl ether **16** (8.35 g, 25 mmol) in THF (150 ml) containing 10% Pd-C (1.09 g) was hydrogenated at 30°C for 16 h. The apparatus was purged with nitrogen and the reaction mixture filtered through silica gel. The crude product was recovered by evaporation of the filtrate (yield 97% as an oil). Recrystallization of this material from hexane gave 5.9 g (94%) of the purified phenol **17**, m.p. 44–45°C, [α]_D²⁰ = +40.9° (c = 1.20; CHCl₃). ¹H NMR (500 MHz, CDCl₃): δ(ppm) 0.96 (s, 3H -CH₃); 1.40 (m, 11H alkyl); 1.75 (m, 2H -C*-CH₂-); 5.20 (s, 1H, -C*-H-); 6.95 (d, 2H-Ar

ortho to -OH); 8.05 (d, 2H-Ar *ortho* to -COOR). MS: *m/z* 250 λ₁ (3.3%) (M⁺), 138 λ₂ (89%), 121 λ₃ (100%), 112 λ₄ (38%). IR (KBr) (cm⁻¹): 3600–3200 (-OH), 1670 (-C=O), 1600 (phenyl ring stretching). EA: C 71.88 (72.0), H 8.73 (8.8)%.

5.3. (S)-(+)-1-Methylheptyl 4-(4-hydroxybenzoyloxy)-benzoate, 3

The compound **18** was obtained by esterification of the acid **14** with the phenol **17** using the dicyclohexylcarbodiimide procedure, but with a reflux time of 4 h followed by stirring at r.t. for 15 h. The crude product was purified by column chromatography using CH₂Cl₂, followed by recrystallization from CH₂Cl₂/C₂H₅OH (1/2) to give 82.3% yield. The intermediate **3** was obtained by hydrogenolysis, the same procedure as used for the benzyl ether **16**. The crude product was crystallized from hexane to give the phenol **3** in a 73% yield, m.p. 170–171°C. ¹H NMR (500 MHz, CDCl₃): δ(ppm) 0.86 (t, 3H, -CH₃); 1.31 (m, 11H alkyl); 1.65 (m, 2H, -CH₂, α to C*); 5.12 (s, 1H, -C*-H); 6.91 (m, 2H ar. *ortho* to -OH); 7.33 (m, 2H ar. *ortho* to -OOC); 8.14 (4H ar. *ortho* -COO). EA: C 71.20 (71.35), H 7.06 (7.03)%.

5.4. (S)-(+)-1-Methylheptyl 4-(4-hydroxybenzoylthio)-benzoate, 4

Thionyl chloride (40 ml) was added to a suspension of 4,4'-dithiodibenzoic acid **20** (4.77 g, 15 mmol) in

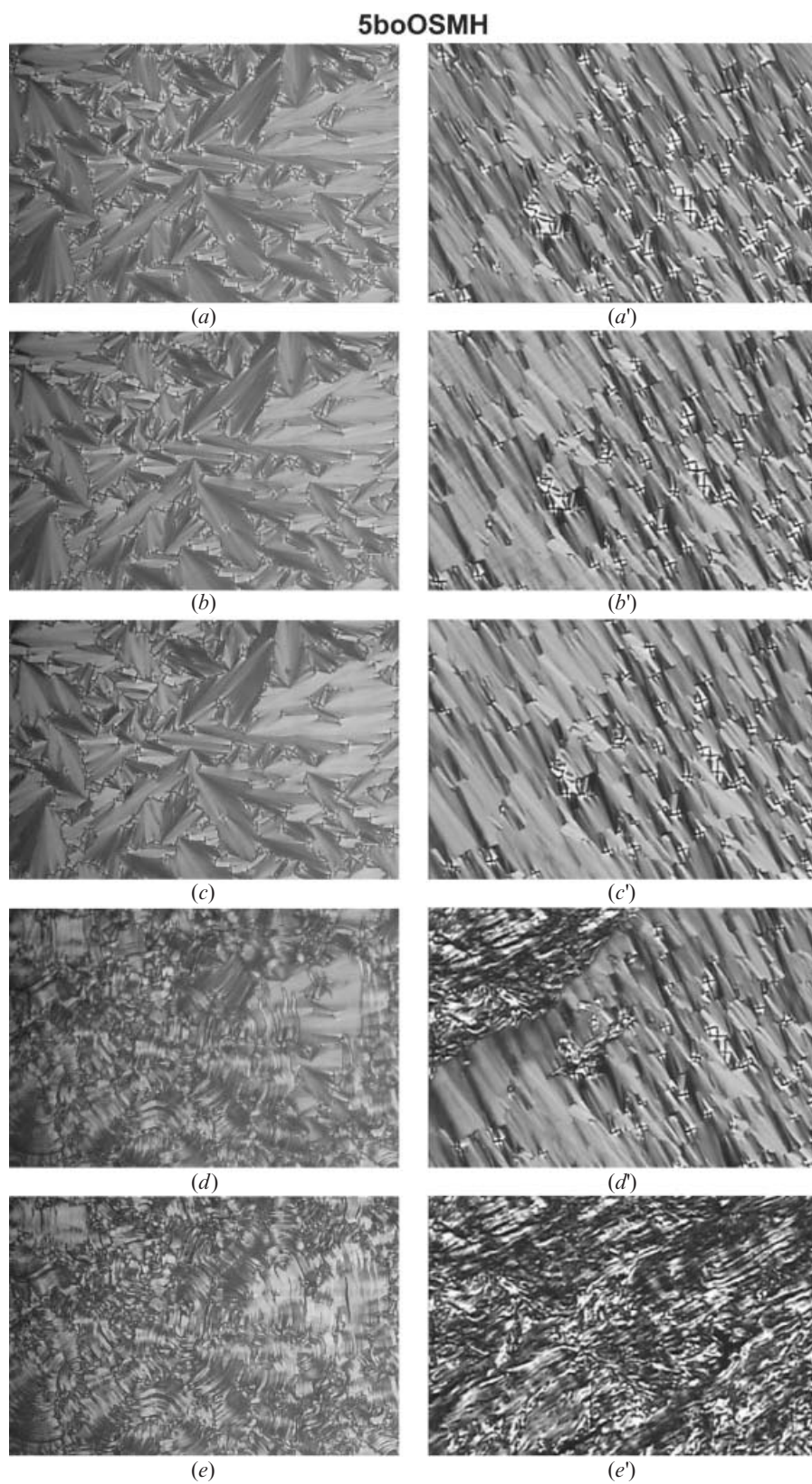


Figure 12. Texture of SmA*, SmB* and Cr phases obtained for compound 5boOSMH in the two types of measurement cell: classical (*a-e*) and Linkam cell (from *a'-e'*). For details see text.

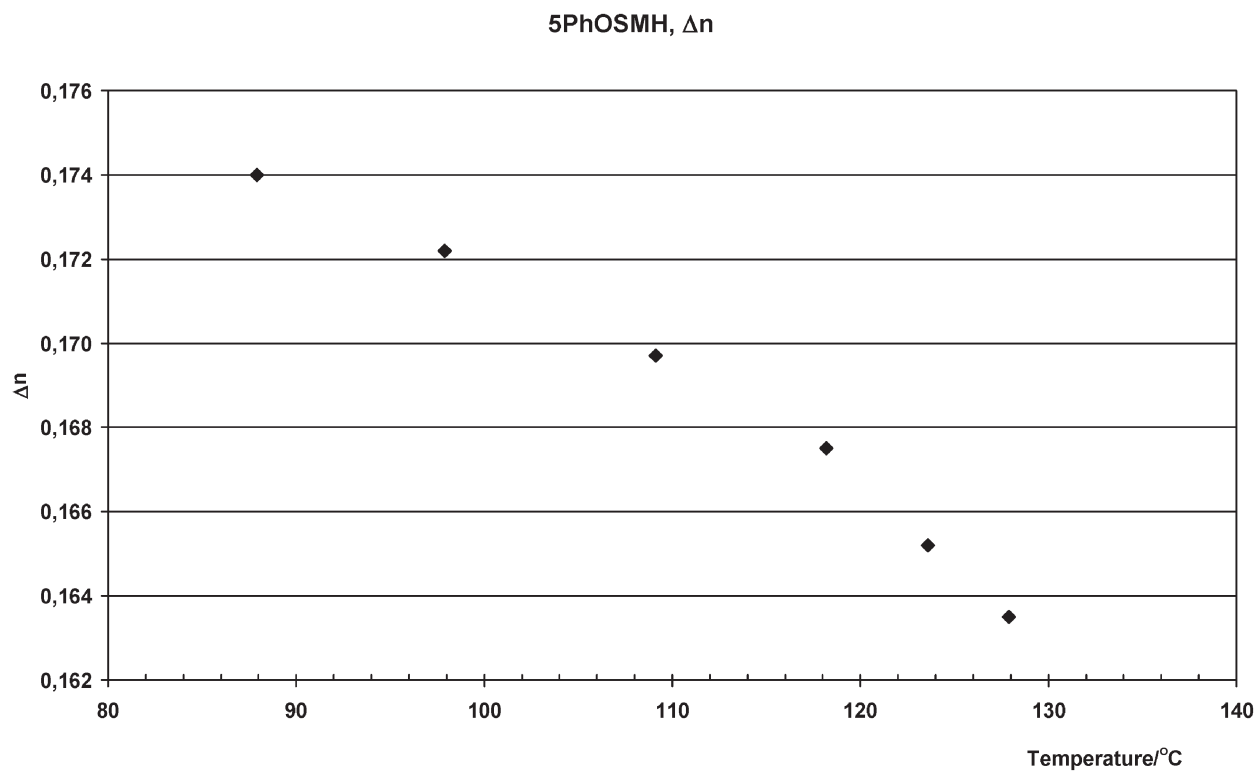


Figure 13. Optical birefringence of 5PhOSMH as a function of temperature.

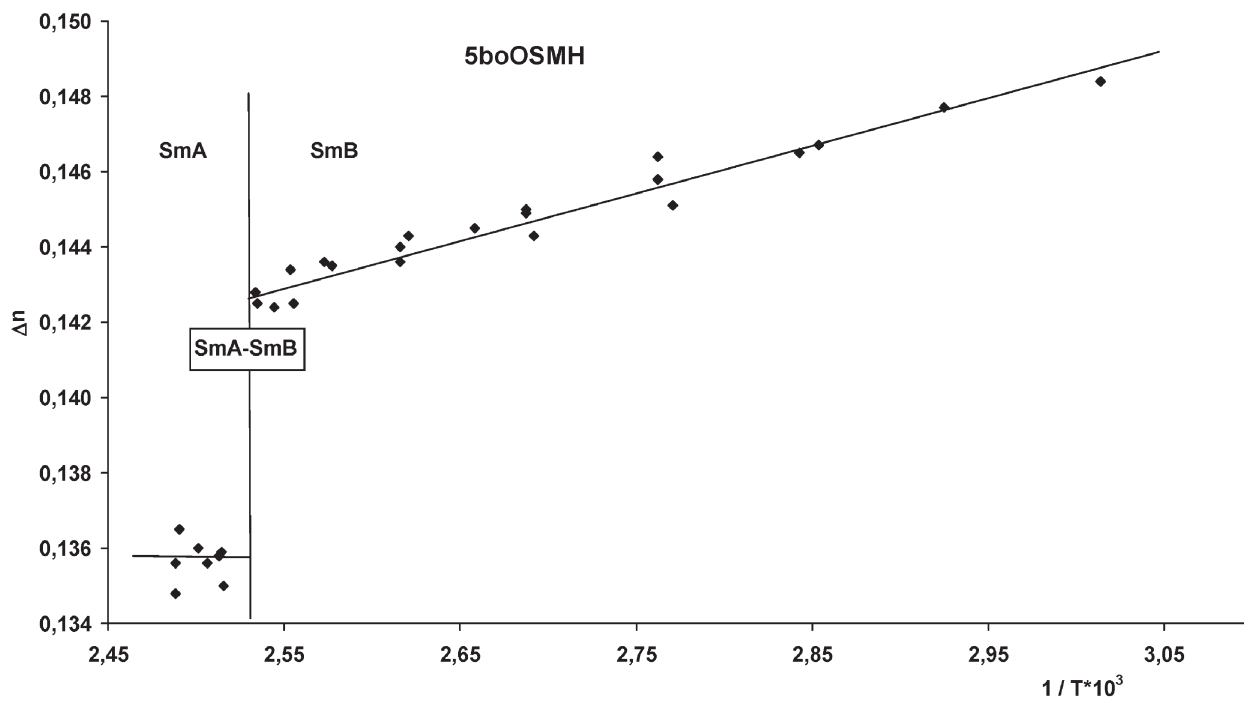


Figure 14. Optical birefringence of 5boOSMH vs. reciprocal temperature.

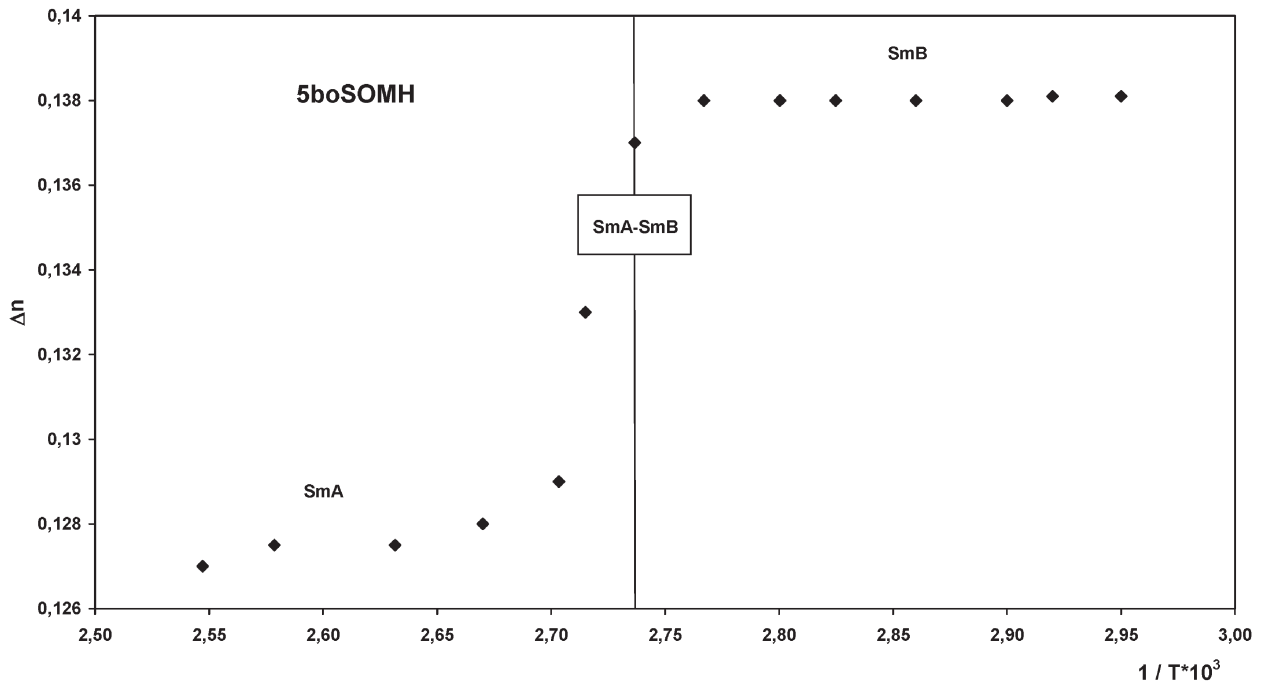


Figure 15. Optical birefringence of 5boSOMH vs. reciprocal temperature.

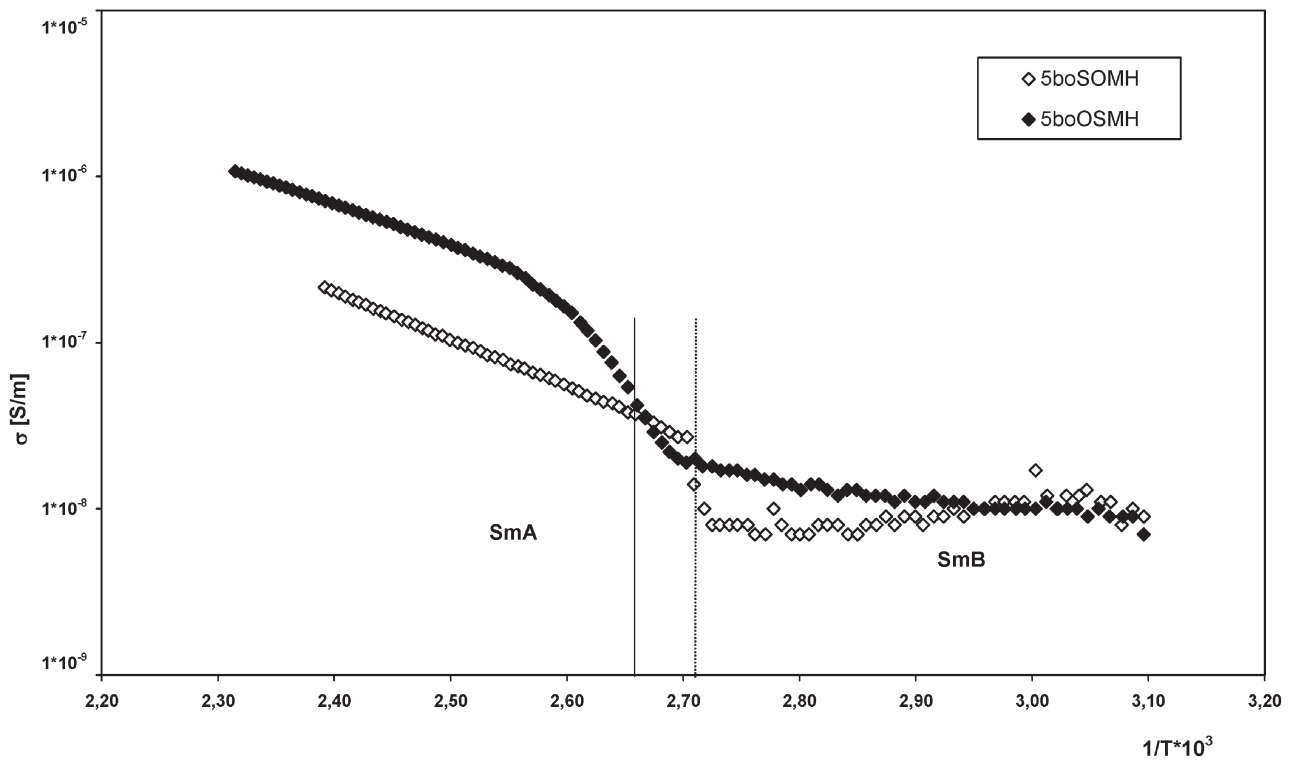


Figure 16. Specific conductivity vs. reciprocal temperature for 5boOSMH and 5boSOMH.

anhydrous toluene (40 ml). The mixture was heated under reflux until dissolution was complete. The mixture was then extracted with hot hexane; the extract was concentrated, and the crude product crystallized from hexane. 4,4'-Dithiodibenzoyl chloride **21** (m.p. 80–82°C) was obtained in 73% yield. ¹H NMR (200 MHz, CDCl₃): δ(ppm) 8.05(m, 4H, *ortho* to –COCl); 7.59(m, 4H, *ortho* to –S–S–).

(*S*)-(+)-2-Octanol (1.54 g, 5 mmol) in toluene (30 ml) was added dropwise to a solution of **21** (1.72 g, 5 mmol) in dry toluene (30 ml) and pyridine (0.45 g, 6 mmol). The mixture was stirred at 35–40°C for 18 h (TLC control, *R_f*=0.48 in CHCl₃). The mixture was filtered, and the filtrate washed with cold water, hydrochloric acid, and again cold water. The toluene layer was dried over anhydrous MgSO₄ and concentrated under vacuum to a yellow oil; this was purified by column chromatography on silica gel using CH₂Cl₂ as eluant. The product **22** was obtained as a light yellow oil (72% yield). ¹H NMR (200 MHz, CDCl₃): δ (ppm) 0.86(t, 6H, –CH₃); 1.29(m, 22H, al); 1.62(m, 4H, –CH₂–); 5.13(s, 2H to C*); 7.50(m, 4H, *ortho* to –S–S–); 7.95(m, 4H, *ortho* to –COO).

Sodium borohydride (0.36 g, 10 mmol) was added in portions to a solution of compound **22** (2.7 g, 5 mmol) in absolute ethanol (70 ml) which was then stirred under nitrogen at r.t. for 1 h (TLC, *R_f* of product 0.62 in CH₂Cl₂). The reaction mixture was added to water with ice and hydrochloric acid and extracted with dichloromethane (3 × 50 ml). The combined dichloromethane layers were washed with water and dried (MgSO₄), filtered, added dry silica gel (2 g) and evaporated to dryness. The silica gel plug was placed on top of a chromatography column and eluted with CH₂Cl₂ under dry argon. Product **23** was obtained as a yellow oil in 93% yield, optical purity 99.5% (HPLC). ¹H NMR (500 MHz, CDCl₃), δ(ppm): 0.98 (t, 3H, –CH₃); 1.39 (m, 11H, alkyl); 1.75 (m, 2H, –C*–CH₂); 3.72 (s, 1H, –SH); 5.18 (s, 1H, –C*H–); 7.10 (d, 2H–Ar *ortho* to –SH), 7.95 (d, 2H–Ar *ortho* to –COOR). IR (KBr, cm^{–1}): 2570 (SH), 1680 (COO), 1600 (phenyl ring stretching). EA (%) calc. for C₁₅H₂₂O₂S, C 67.67, H 8.27, S 12.03; found C 67.70, H 8.23, S 12.00.

Compound **23** (2.7 g, 10 mmol) in anhydrous methyl chloride (30 ml) was slowly added to a solution of 4-methoxycarbonylbenzoyl chloride (2.1 g, 10 mmol) with pyridine (0.8 g, 10.1 mmol) in CH₂Cl₂ (30 ml). The mixture was stirred at r.t. for 12 h under dry argon. The product **24** was isolated and purified by typical methods and was obtained as an oil in 81% yield.

Aqueous Ammonia (28%, 50 ml) was added to a solution of compound **24** (3.7 g, 8.5 mmol) in isopropanol (50 ml), and the reaction mixture was stirred at 10°C

for 2.5 h (TLC control). The mixture was added to 150 ml water with ice and 3 ml HCl; the insoluble solid was removed by filtration, washed with water and dried. The crude product was purified by flash chromatography using CH₂Cl₂ and was recrystallized from hexane to give 2.5 g of phenol **4** in 78% yield, m.p. 116–117°C. ¹H NMR (500 MHz, CDCl₃), δ (ppm): 0.87 (t, 3H, –CH₃); 1.33 (m, 11H, alkyl); *5.06 (s, 1H, –C*H–); 6.90 (s, 1H, –OH) 7.05 (d, 2H, *ortho* to –OH); 7.56 (d, 2H, *ortho* to –SOC–); 8.00 (d, 2H, *ortho* to –COS–); 8.30 (d, 2H, *ortho* to –COOR*). IR (KBr, cm^{–1}): 3393, 2931, 2857, 1716, 1682, 1600, 1580, 1511, 1284, 1209, 1164, 901, 842, MS (*m/z*, %): 387(M⁺+1, 2,50), 121(M⁺–266, 100,00), 136 (M⁺–250, 89,30). EA (%) calc for C₂₂H₂₆O₄S C 68.39, H 6.74, S 8.29; found C 68.41, H 6.79, S 8.26.

5.5. (*S*)-(+)-1-Methylheptyl 4-(4-mercaptobenzoyloxy)-benzoate, **5**

Pyridine (22 mmol) was added to a solution of 4,4'-dithiodibenzoyl chloride **21** (3.55 g, 10 mmol) in toluene (50 ml), stirred for 10 min and added slowly to a solution of compound **17** in toluene (40 ml) and stirred at 40–45°C for 18 h. The crude product **25** was isolated in the same way as **22**. The white product **25** was recrystallized from methyl chloride/ethyl alcohol (1/2), m.p. 113–115°C; a yield of 67% was achieved. ¹H NMR (500 MHz, CDCl₃): δ (ppm) 0.87 (t, 6H, –CH₃); 1.3 (m, 22H, alkyl); 1.63 (m, 4H, –CH₂–) α to C*); 5.15 (s, 2H to C*); 7.27 (m, 4H, *ortho* to –OOC); 7.65 (m, 4H, *ortho* to –S–S–); 8.13 (8H, *ortho* to –COO).

Sodium borohydride (0.189 g, 5 mmol) was added quickly to a solution of compound **25** (3.7 g, 5 mmol) in absolute ethanol (70 ml) and the mixture stirred under nitrogen at room temperature for 50 min (TLC control, *R_F* of product 0.28 in CHCl₃). The reaction mixture was added to water with ice and hydrochloric acid and extracted with dichloromethane (3 × 50 ml). The combined dichloromethane layers were washed with water and dried (MgSO₄); the solution was filtered, dry silica gel (2 g) added and evaporated to dryness. The silica gel plug was placed on top of a chromatography column and eluted with CH₂Cl₂. The intermediate **5** was obtained in a yield of 71%, m.p. 54.0–54.5°C. ¹H NMR (500 MHz, CDCl₃): δ(ppm) 0.9(t, 3H, –CH₃); 1.29(m, 11H, alkyl.); 3.99(s, 1H, –SH); 5.11(s, 1H, to C*); 6.91(d, 2H, *ortho* to –SH); 7.73(d, 2H, *ortho* to –OOC); 8.05(d, 2H, *ortho* to –COOR); 8.35(d, 2H, *ortho* to –COO–Ar). MS (*m/z*, %): 387 (M⁺+1, 18.1); 136 (M⁺–250, 100.0); 250 (M⁺–136, 52.7); 120 (M⁺–266, 61.2). EA for C₂₂H₂₆O₄S: calcd C 68.39, H 6.74, S 8.29; found C 68.32, H 6.79, S 8.28%.

5.6. General procedure for the preparation of compounds 6–11

Dry pyridine (10 mmol) was added to a solution of 10 mmol of compound **1** or **2** in 40 ml dry dichloromethane and stirred for 5 min. A solution of 10 mmol of compound **3**, **4** or **5** in 30 ml dry dichloromethane was added to this mixture. The reaction mixture was stirred at room temperature for 10–15 h. As soon as TLC analysis revealed completion of the reaction, the reaction mixture was cooled to 10°C and added to water with ice and hydrochloric acid (15 ml, 15%). The dichloromethane layer was washed several times with water and aqueous sodium carbonate. The organic phases were dried over anhydrous MgSO₄ and then filtered. Solvent was evaporated from the filtrate; the residue was purified by column chromatography on silica gel using CH₂Cl₂ as eluant to give a white solid. This was recrystallized from absolute ethanol to give white crystals of compounds: **6** (80.6%), **7** (82.5%), **8** (73.4%), **9** (79.2%), **10** (65.7%) and **11** (70.1%).

6: ¹HNMR (500 MHz, CDCl₃, δ ppm): 0.90 (m, 6H, –CH₃); 1.29 (m, 16H, –CH₂–, alkyl); 1.34 (d, –CH₃ to C*); 1.42 (m, 2H, –CH₂– α to C*); 1.67 (m, 12H, bo-ring); 5.17 (s, 1H, –C*H–); 7.45 (m, 4H, *ortho* to –OCO–); 8.14 (m, 4H, *ortho* to –CO). IR (KBr, cm^{–1}): 2927, 2860, 1746, 1738, 1711, 1600, 1505, 1263, 1193, 1161, 1063, 1063, 977, 759. MS (*m/z*, %): 576 (M⁺, 1), 207(100), 120(89). EA (%) calc. for C₃₆H₄₈O₆ C 75.00, H 8.33; found C 75.06, H 8.30.

7: ¹HNMR (500 MHz, CDCl₃, δ ppm): 0.98 (m, 6H, –CH₃); 1.57 (m, 19H, alkyl); 2.70 (t, 2H, –CH₂–Ar); 5.24 (s, 1H, –C*H); 7.55 (d, 2H, *ortho* to –CH₂–); 7.78 (m, 4H, *ortho* to –OCO); 8.20–8.40 (m, 6H, *ortho* to –CO). IR (KBr, cm^{–1}): 2928, 2854, 1738, 1721, 1701, 1602, 1508, 1462, 1414, 1264, 1203, 1162, 1059, 1015, 890, 758. MS (*m/z*, %): 544 (M⁺, 2), 121 (100), 147(79). EA (%) calc. for C₃₄H₄₀O₆ C 75.00, H 7.35; found C 74.98, H 7.38.

8: ¹HNMR (500 MHz, CDCl₃, δ ppm): 0.89 (m, 6H, –CH₃); 1.26 (m, 16H, –CH₂–); 1.35 (d, 3H –CH₃ to C*); 1.46 (m, 2H, –CH₂– α to C*); 1.70 (m, 12H, bo-ring); 5.19 (s, 1H, –C*H); 7.27 (d, 2H, *ortho* to –SCO); 7.53 (d, 2H, *ortho* to –OCO); 8.12 (d, 2H, *ortho* to –COOAr); 8.19 (d, 2H, *ortho* to –COOC*). IR (KBr): 2925, 2859, 1741, 1710, 1667, 1598, 1457, 1409, 1269, 1203, 1166, 1112, 902, 762. MS (*m/z*, %): 592 (M⁺, 2), 207 (100), 120 (91). EA (%) calc. for C₃₆H₄₈O₅S C 72.97, H 8.11, S 5.41; found C 73.00, H 8.09, S 5.42.

9: ¹HNMR (500 Hz, CDCl₃, δ ppm): 0.90 (m, 6H, –CH₃); 1.62 (m, 19H, alkyl); 2.73 (t, 2H, –CH₂–Ar); 5.20 (s, 1H, –C*H); 7.51 (d, 2H *ortho* to –CH₂–); 7.60 (d, 2H *ortho* to –SCO); 7.70 (d, 2H *ortho* to –OOC–Ar); 8.19 (d, 2H *ortho* to –COOC*–); 8.30 (d, 2H *ortho* to –COS–);

8.39 (d, 2H *ortho* to –COOAr). IR (KBr, cm^{–1}): 2926, 2856, 1743, 1719, 1667, 1596, 1460, 1404, 1274, 1227, 1166, 1113, 1073, 906, 761. MS (*m/z*, %): 560 (M⁺, 2), 147 (91), 121 (100). EA (%) calc. for C₃₄H₄₀O₅S C 72.89, H 7.14, S 5.74; found C 72.89, H 7.12, S 5.73.

10: ¹HNMR (500 MHz, CDCl₃, δ ppm): 0.93 (m, 6H, –CH₃); 1.29 (m, 16H, –CH₂–); 1.40 (d, 3H, –CH₃ to C*); 1.49 (m, 2H, –CH₂–, α to C*); 1.76 (m, 12H, bo-ring); 5.21 (s, 1H, –C*H); 7.20 (d, 2H, *ortho* to –SCO); 7.49 (d, 2H, *ortho* to –OCO); 8.16 (d, 2H, *ortho* to –COOAr); 8.23 (d, 2H, *ortho* to –COOC*). IR (KBr, cm^{–1}): 2927, 2858, 1748, 1717, 1667, 1594, 1456, 1410, 1272, 1206, 1165, 1111, 1040, 903, 755. MS (*m/z*, %): 592 (M⁺, 2), 207 (100), 121 (93). EA (%) calc. for C₃₆H₄₈O₅S C 72.97, H 8.11, S 5.41; found C 72.99, H 8.09, S 5.40.

11: ¹HNMR (500 Hz, CDCl₃, δ ppm): 0.94 (m, 6H, –CH₃); 1.42 (m, 19H, alkyl); 2.80 (t, 2H, –CH₂–Ar); 5.23 (s, 1H, –C*H); 7.40 (d, 2H, *ortho* to –SCO); 7.51 (d, 2H, *ortho* to –CH₂–); 7.64 (d, 2H, –OCO); 8.15 (d, 2H, *ortho* to –COOC*); 8.24 (d, 2H, *ortho* to –COS), 8.30 (d, 2H, *ortho* to –COO). IR (KBr, cm^{–1}): 2926, 2855, 1738, 1718, 1675, 1605, 1460, 1411, 1264, 1210, 1162, 1114, 1068, 1015, 905, 758. MS (*m/z*, %): 560 (M⁺, 2), 147 (100), 121 (93). EA (%) calc. for C₃₄H₄₀O₅S C 72.86, H 7.14, S 5.71; found C 72.83, H 7.15, S 5.70.

6. Conclusion

The synthesis of six new compounds with chiral terminal chains and three-ring molecules has been described in detail. These compounds have either two benzene rings and one bicyclo[2,2,2]octane or three benzene rings with –COS– and –COO– bridging. Replacing the –COO– bridge with –COS– increases thermal stability of the compounds. In mesogenes of the **B** series the change of the –COS– bridge does not generate new phases. One can observe the influence of the location of the bridge on the phase transition temperatures. In the **A** series the –COS– bridge leads to the formation of an enantiotropic SmB* phase. The location of the –COS– bridge influences the formation of a supercooled glassy state. When comparing the properties of series **A** and **B** compounds, a distinct influence of the bicyclo[2,2,2]octane ring on phase polymorphism can be seen.

All the six compounds have an enantiotropic SmA* phase. Compound 5boOOMH (**6**) has enantiotropic SmA* and monotropic SmB* phases. Its analogue 5PhOOMH (**7**) has only an enantiotropic SmA* phase. Compounds 5PhOSMH (**9**) and 5PhSOMH (**11**) also have an enantiotropic SmA* phase. Compounds 5boOSMH (**8**) and 5boSOMH (**10**) have enantiotropic SmA* and SmB* phases.

In all the substances studied, the smectic layer spacing d and optical birefringence Δn , as well as their differences between the SmA* and SmB* phases, were shown to be influenced by the position of the –COO– and –COS– linking groups and by the type of rings present in the molecules (one bicyclo[2,2,2] octane or all phenyl).

Acknowledgements

Prof. Jan Przedmojski, Warsaw University of Technology, Poland is thanked for X-ray measurements. I would like to thank Wojciech Zajac for discussions during preparation of the manuscript. This work was partly supported by the Polish Ministry of Scientific Research and Information Technology, Grant No.4 T09A 200 25.

References

- [1] G.W. Gray, S.M. Kelly. *Chem. Commun.*, 465 (1980).
- [2] G.W. Gray, S.M. Kelly. *J. chem. Soc. Perkin II*, 267 (1981).
- [3] N. Carr, G.W. Gray, S.M. Kelly. *Mol. Cryst. liq. Cryst.*, **66**, 267 (1981).
- [4] N. Carr, G.W. Gray, D.G. McDonnell. *Mol. Cryst. liq. Cryst.*, **97**, 13 (1983).
- [5] R. Dąbrowski, J. Dziaduszek, W. Drzewiński, K. Czupryński, Z. Stolarz. *Mol. Cryst. liq. Cryst.*, **191**, 171 (1990).
- [6] R. Dąbrowski, J. Dziaduszek, T. Szczuciński, Z. Stolarz, K. Czupryński. *Liq. Cryst.*, **5**, 1, 209 (1989).
- [7] R. Dąbrowski, J. Dziaduszek, J. Szulc, K. Czupryński, B. Sosnowska. *Mol. Cryst. liq. Cryst.*, **209**, 201 (1991).
- [8] D. Demus, H. Demus, H. Zschke. *Flüssige Kristalle in Tabellen Vols I, II* (1974, 1984).
- [9] E. Campaigne, W.W. Meyer. *J. org. Chem.*, **27**, 2835 (1962).
- [10] Y.H. Kim, Y. Gaumont, R.L. Kisliuk, H.G. Mautner. *J. med. Chem.*, **18**, 776 (1975).
- [11] J.M. Domagala, J.P. Bader, R.D. Gogliotti, J.P. Sacher, M.A. Stier, Y. Song, J.V.N. Vara Prasad, P.J. Tummino, J. Scholten, P. Harvey, T. Holler, S. Gracheck, D. Hupe, W.G. Rice, R. Schultz. *Bioorg. med. Chem.*, **5**, 596 (1997).
- [12] A. Gangiee, R. Devraj, J.J. McGuire, R.L. Kisliuk. *J. med. Chem.*, **38**, 4495 (1995).
- [13] S.L. Wu, C.Y. Lin. *Liq. Cryst.*, **30**, 471 (2003).
- [14] J. Chruściel, B. Pniewska, M.D. Ossowska-Chruściel. *Mol. Cryst. liq. Cryst.*, **258**, 325 (1995).
- [15] Z. Karczmarzyk, M.D. Ossowska-Chruściel, J. Chruściel. *Mol. Cryst. liq. Cryst.*, **357**, 117 (2001).
- [16] M.D. Ossowska-Chruściel, Z. Karczmarzyk, J. Chruściel. *Mol. Cryst. liq. Cryst.*, **382**, 37 (2002).
- [17] K. Hori, S. Kawahara, K. Ito. *Ferroelectrics*, **147**, 91 (1993).
- [18] K. Hori, K. Endo. *Bull. chem. Soc. Jpn.*, **66**, 46 (1993).
- [19] R. Dąbrowski, K. Czupryński, J. Przedmojski, B. Ważyńska. *Liq. Cryst.*, **14**, 1359 (1993).
- [20] M.D. Ossowska-Chruściel, S. Zalewski, A. Rudzki, A. Feliks, J. Chruściel. *Phase Transitions* (in press).